Acoustic Detection of Extremely High Energy Cosmic Ray Neutrinos: Results from an Undersea Microphone Array

Submitted to the Department of Physics of Stanford University
in Partial Fulfillment of the Requirements
for the Degree of Bachelor of Science

Justin Vandenbroucke
May 2002

ABSTRACT

The cosmic ray spectrum at its extremely high energy tail, 10^{20} eV, is an outstanding mystery in current physics. Several cosmic rays have been detected at this energy, but their origin and identity remain unknown. This unsolved mystery lies at the intersection of several exciting topics in astrophysics and particle physics. The cosmic ray flux at this energy is roughly 1/km^2/century, so very large detectors are necessary to study the problem. Detection in water, based on the fact that these particles are energetic enough to make a sound when they hit the sea, has been discussed for decades, but the method's potential remains unclear. In the past year an existing array of undersea microphones operated by the United States Navy has been equipped with a data acquisition system and has collected data for several months. The background rate and energy threshold for detection with this method have been determined.

INTRODUCTION

In 1912, Victor Hess, ascending to an altitude of 5 km in a balloon, discovered that the level of radioactivity increased with altitude. This was quite a surprise, as previous experiments at the Eiffel Tower had shown a decrease in radioactivity with height. The source of the radioactivity was thought to be rocks in the earth. Hess's work, however, indicated a new, extraterrestrial, source of radioactivity. Robert Millikan called them "cosmic rays." Since their discovery, the energy and composition (identity) of cosmic rays has been explored in great depth and is generally well understood. Like cathode rays before them, they were shown to be familiar particles (protons, electrons, and atomic nuclei) rather than fundamental new particles.[1] Cosmic rays proved fertile ground for the study of particle physics. In the 1930's and 1940's, physicists studying cosmic rays discovered muons, K mesons and hyperons (the first particles containing a strange quark), and all three pions.[2] Today, revolutionary measurements of neutrino mass and oscillation are being made with neutrinos produced in the atmosphere by cosmic rays.

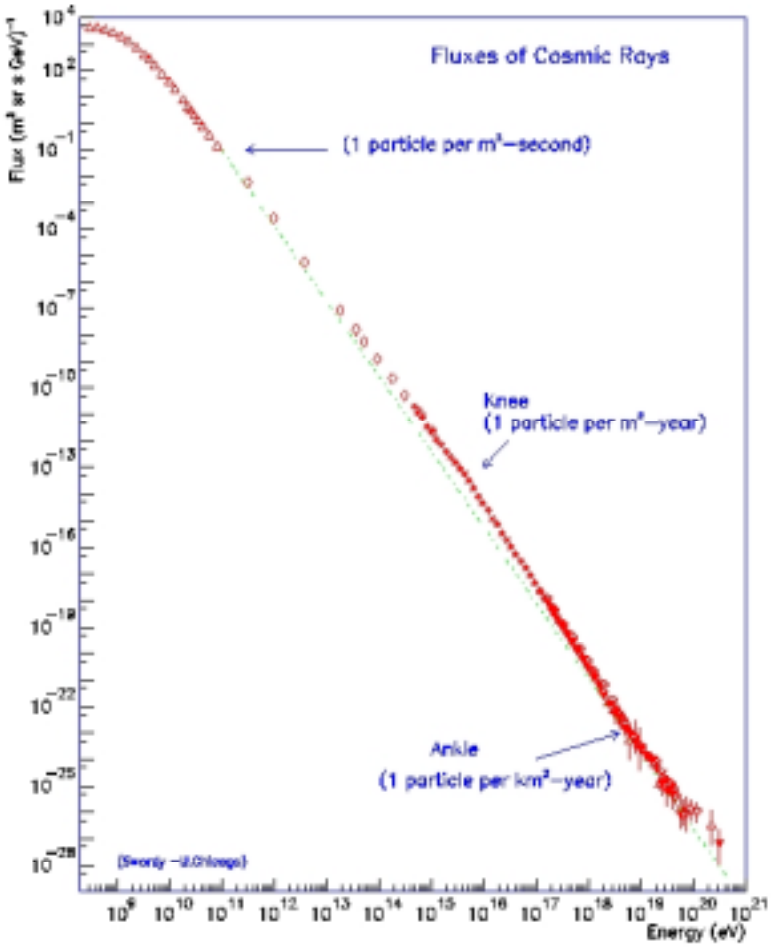

Figure 1. The cosmic ray spectrum above a GeV.[3] The flux roughly follows a power law of index -3.

The energy spectrum of the particles has been measured precisely (Figure 1). The highest-energy cosmic rays, however, remain an enigma. As Greisen, Zatsepin, and

Kuz'min (GZK) realized in 1966[4], a cosmic ray nucleus propagating through space should interact with the photons of the cosmic microwave background (CMB), producing pions according to the reaction $N_1\gamma \rightarrow N_2\pi^+$, where the N_i are nucleons, and N_1 may or may not equal N_2 (the fundamental interaction is $p\gamma \rightarrow p\pi^0$ or $p\gamma \rightarrow n\pi^+$). This process, known as photo-pion production, effectively lowers the energy of the cosmic ray. The mean free path for a 10^{20} eV cosmic ray in the CMB is 50 Mpc. Nucleons at this energy should not generally be able to propagate farther than this distance. This effect is known as the GZK cutoff.

At least ten events above 10^{20} eV have been detected by the Akeno Giant Air Shower Array (Figure 2).[5] If they are atomic nuclei or protons, they should have originated within 50 Mpc. However the events do not point back to astrophysical objects capable of accelerating particles to such a high energy within this distance.

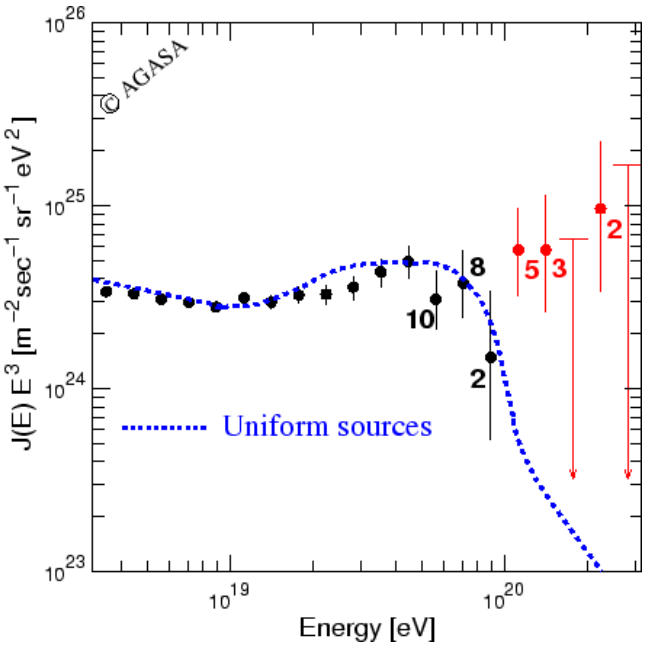

Figure 2. The extremely high energy cosmic ray spectrum, as measured by AGASA.[6] The general power-law trend has been removed by multiplying by E^3. The dotted blue line indicates the expected spectrum due to the GZK effect with extragalactic astrophysical sources uniformly distributed throughout the universe.

A wealth of theories has been proposed to explain the GZK anomaly. These theories generally fall into two categories. Astrophysical ("bottom-up") theories claim that the extremely high energy cosmic rays (EHECR, energy greater than 10^{18} eV) are standard particles accelerated to extreme energies by exotic astrophysical phenomena. These sources include active galactic nuclei (AGN) and gamma ray bursts (GRB). Particle ("top-down") theories claim that the particles are decay products of as-yet undiscovered particles. Top-down theories variously explain the GZK anomaly with dark matter, supersymmetry, super-heavy Big Bang relics, axions, and topological defects (monopoles, cosmic strings, and domain walls). The anomaly could also be explained by Lorentz invariance violation.[7]

It should be emphasized that 10^{20} eV is an exceedingly high energy: it is the energy of a golf ball moving at 40 mph, but in a single sub-atomic particle. This energy is 100 million times the largest energy produced at manmade particle accelerators. The center-of-mass energy of EHECR collisions with nucleons in the Earth is PeV-scale. No cross sections have been experimentally measured at this energy for any interactions, including the neutrino-nucleon interaction. An advanced EHECR detector could measure this cross section (in addition to measuring the EHECR flux), constraining the standard model (SM) predictions.

Many current theories, including those of extra dimensions and loop quantum gravity, predict deviations from the SM at PeV energies. In particular, if the scale for gravity unification with the other forces is at a TeV (as it is according to recent large-extra-dimensions theories), then an incident EHECR can approach an earthbound nucleon closer than its Schwarzchild radius, creating a small black hole[8]. The black hole decays instantaneously into Hawking radiation. It has been speculated that through this mechanism EHECR detectors may be able to find extra dimensions (if they exist) before accelerators.

EHECR therefore have the potential to be an excellent tool for the exploration of exotic astrophysics and particle physics. The detection and identification of EHECR is, however, a formidable challenge. Because their flux is roughly 1/km^2/century, a detector of at least 100 km^2 is necessary for a reasonable event rate.

DETECTORS

When a high-energy particle hits the Earth, it interacts with a quark to produce a secondary high-energy particle. These interactions cascade, producing a shower. At extremely high energies, particles other than neutrinos shower high in the atmosphere, while neutrinos more often penetrate the atmosphere and shower in land or sea. There are therefore two types of detectors: those detecting non-neutrinos that shower in the air, and those detecting neutrinos that shower in ice or water.

Three methods have been used to detect air showers: direct ground detection, nitrogen fluorescence, and Cerenkov radiation. Ground arrays are arrays of standard charged-particle detectors on the ground. They detect showers that occur low in the atmosphere or high in the atmosphere with enough energy to reach the ground. Nitrogen fluorescence detectors detect fluorescence emitted by nitrogen atoms in the atmosphere excited by charged particles in the shower. Cerenkov (optical) detectors detect the radiation produced by high-speed charged particles in the shower.

At extremely high energies, undersea and under-ice detectors only detect neutrinos. This is not a strong impediment as a significant EHE neutrino flux is predicted even if the primary EHECR are atomic nuclei. "Cosmogenic" neutrinos are guaranteed if the primary EHECR are nuclei: They are the decay products of pions produced by the nuclei interacting with the CMB ($\pi^+ \rightarrow e^+ \nu_e \nu_\mu \bar{\nu}_\mu$). Several theories also predict that a component of the primary cosmic rays are neutrinos. A detector that only detects neutrinos is therefore quite useful.

Undersea and under-ice detectors have thus far been arrays of optical Cerenkov detectors spaced tens of meters apart. It is very difficult to achieve an effective area of 100 km^2 with this spacing.

ACOUSTIC DETECTION

When an EHE neutrino showers in the sea, the shower particles eventually deposit their energy in the water as heat. This heat causes the water to expand, resulting in an acoustic wave. The frequency of the wave is broadband but peaked at roughly 10 kHz. The shape of the wave is predicted to be a simple bipolar pulse. Acoustic radiation by charged particles in water is well understood theoretically[9] and has been demonstrated experimentally[10] with bunches of 200 MeV protons with total energy $10^{19\text{-}21}$ eV.

The heat deposition is roughly cylindrical along the shower. Because the source is long and thin, the acoustic radiation is emitted in a very thin, wide disk perpendicular to the incident neutrino path. Although the anisotropy is an advantage for direction reconstruction, the thinness of the disk limits the effective volume for detection.

The divergence of the signal is significantly less than that from a point source. Moreover, the attenuation length of acoustic waves is roughly ten times that of light in seawater. It is therefore possible that an acoustic array of detector modules could be much sparser and cover much more area per dollar than optical modules, making larger detectors feasible.

Figure 3. The Tongue of the Ocean is clearly seen as very dark water in this satellite image. Andros Island is west of the tongue. The hydrophone array spans the thin part of the tongue.

THE AUTEC DETECTOR

The U. S. Navy operates an array of hydrophones (underwater microphones), the Atlantic Undersea Testing and Evaluation Center (AUTEC), in the Tongue of the Ocean (TOTO) off the coast of Andros Island in the Bahamas (Figure 3). The Tongue of the Ocean is a very deep groove in which 1-2 km depths are attained within several km of shore, making it practical to lay cables from a deep sea floor to shore for processing. There is also very little shipping traffic, making it a quiet location for acoustic work. The AUTEC facilities consist of the hydrophone array along with several sites on Andros Island. AUTEC is used by the U.S. and British navies for testing new weapons and

training personnel. Use of the array consists of "tests" involving ships, planes, submarines, and/or torpedoes. The array is optimized to track submarines and torpedoes that emit specific and regular pinger signals.

The array contains 62 hydrophones, each held by a boom roughly 5 m above the seafloor, 1.5 km below the surface (suspension halfway between floor and surface would be better for our purpose). Most have a separation of 3 km, but 8 hydrophones are arrayed in equilateral triangles with a separation of 1.5 km (the "fine tracking array"). Frequencies in the band 7.5-50 kHz are passed by the hydrophones (also passing the component below 7.5 kHz would be ideal for neutrino signals).

As a well-calibrated and well-understood array that has operated successfully for 30 years, AUTEC is a good site for a feasibility study. We have established an agreement with the U.S. Navy under which we can use the array whenever the Navy is not conducting a test. Tests typically occur between 6am and 5pm on most but not all weekdays. In practice we are able to run 75% of the time.

In April 2001 a study was proposed using the array[11]. A data acquisition system has been installed and upgraded during two trips to the site in August and December of 2001. The system is running with seven of the eight fine-tracking hydrophones, as shown in Figure 4. This sub-array covers an area of 7 km^2. The entire AUTEC array covers roughly 250 km^2.

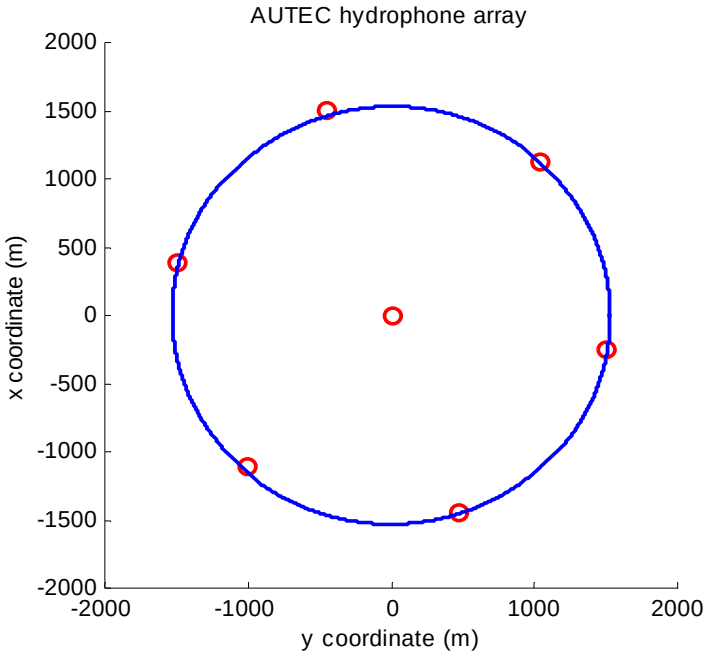

Figure 4. Geometry of the detector used in this study. The blue circle indicates our fiducial area.

DATA ACQUISTION

The data acquisition (DAQ) system is installed at AUTEC Site 3, one of several sites where cables come ashore from the array and lead to a small building with signal processing hardware. Site 3 is on Big Wood Cay, an island covered almost entirely by dense brush and with a population of 5 (all Navy employees).

BNC cables carrying analog signals from each of the seven hydrophones feed into a digital I/O board (National Instruments PCI-MIO-16E) that digitizes the seven signals at 179 kHz each and sends them to a single PC (Dell 8100, 1.7 GHz Pentium 4).

There is a small DC offset in each channel, and the hydrophones have different but constant gains. As of the December 2001 upgrade, the DC offset is removed and the voltage levels are rescaled online before processing.

The data acquisition algorithm is a two-level trigger. The first level is a digital matched filter. The purpose of the digital filter is to indicate when the signal is similar in shape to that predicted for neutrinos. The response function for the digital filter is shown in Figure 5. If the filtered voltage is above threshold, a level-1 trigger occurs.

Because the sea conditions are highly variable, an adaptive threshold is used: A target event rate of 1 Hz is set and the threshold is raised or lowered each minute by a constant increment to seek this rate. The threshold is the same for each hydrophone. With this scheme more events are captured in quiet conditions and we are not swamped during noisy conditions. In practice, this algorithm results in periods of relatively constant threshold punctuated by periods of elevated threshold, presumably the result of varying weather conditions and biological activity. A relatively large threshold step size is used to limit the number of thresholds used (three thresholds are used for more than half of the time). The distribution of thresholds is shown in Figure 6.

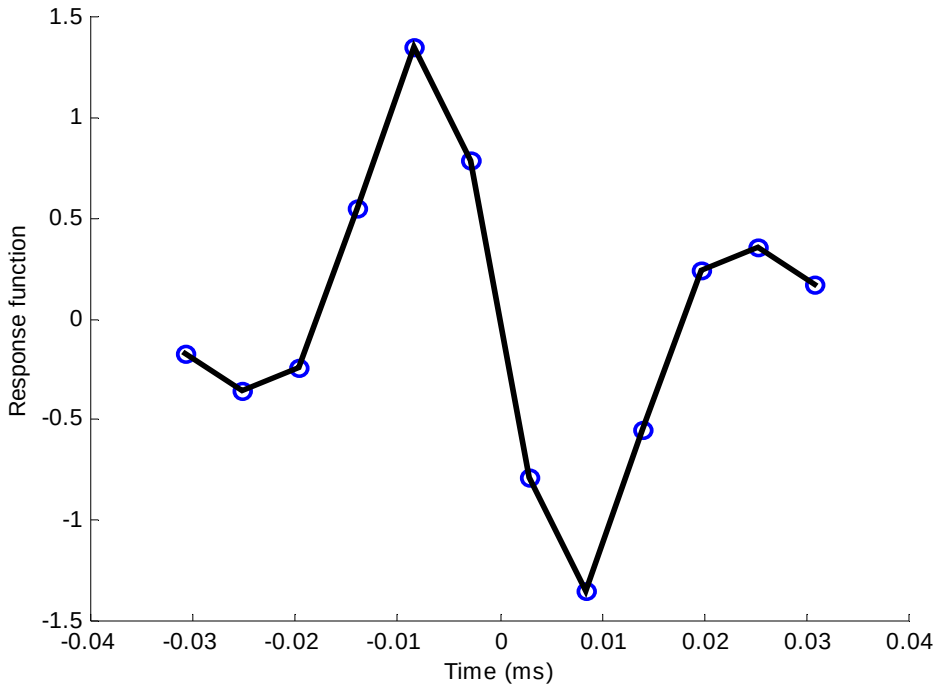

Figure 5. The response function used in the digital matched filter (arbitrary units).

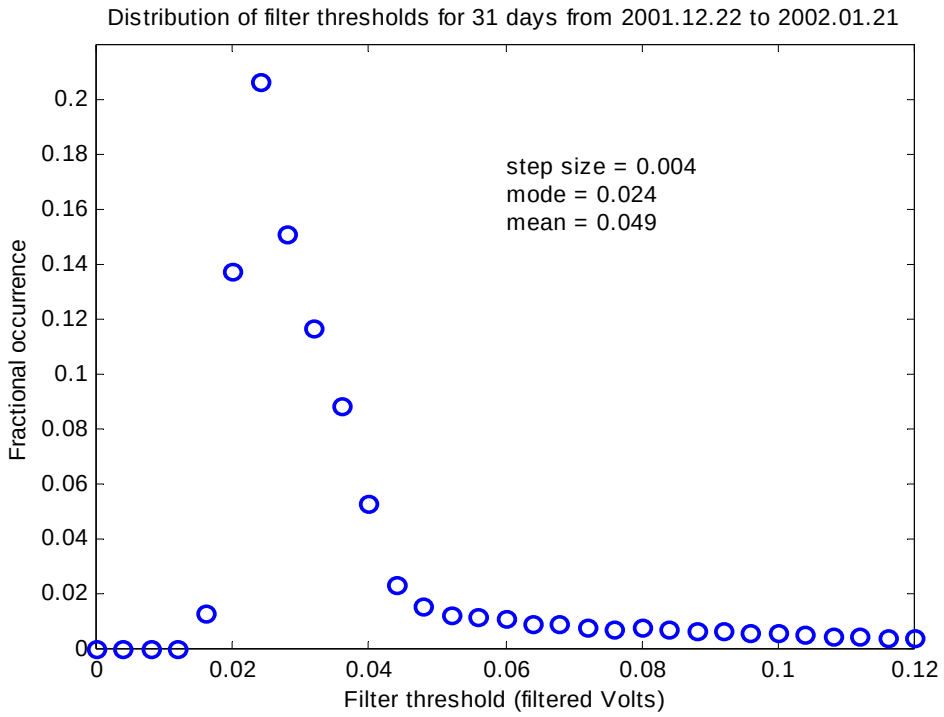

Figure 6. Distribution of the single-phone detection threshold using the filter algorithm with adaptive threshold, as determined from 31 days of data. Units are volts after filtering, where the voltage level of each channel represents the pressure at one phone. The histogram bins are equal to the actual values used as thresholds. Note that most of the time the threshold is one of only 3 values. Note also the long tail of the distribution, giving a mean value twice as high as the most probable.

After level-1 triggering, roughly one third of the events are 7.5 kHz signals highly correlated among channels. The channels are correlated on the μs scale. For an actual acoustic source producing a signal propagating at 1.5 km/s through seawater to detectors with km-scale separation, we expect the actual signal arriving at two phones to be separated in time by of order one second. Therefore the highly correlated events are thought to be due to electronic noise. A level-2 trigger, installed in the December 2001 upgrade, removes these events by cutting on the sum of the correlation of each of the 21 pairs of channels.

A data file is written each minute, containing summary data for the minute in addition to data for each triggered event during that minute. Minute summary data include an estimate of the noise spectrum, the threshold value for that minute, and, every 10 minutes, a 100 ms 7-channel time series recorded at the beginning of the minute (this is useful as a sample of non-triggered background noise).

Data for each event include a time stamp, an integer representing which phone triggered, and a seven-channel time series. Capturing all seven channels allows for further removal of electronic-noise events offline. Nine-tenths of triggered time series are 1 ms (179 samples) long; one-tenth are 10 ms (1790 samples) long. The expected neutrino signal is roughly 0.1 ms long. The long acquisitions are taken to search for acoustic reflections off the sea floor following the primary signal. These bottom reflections (occurring within 10 ms of the primary signal) help constrain the source

position for reconstruction, but capturing 10 ms for every event would exceed our data handling capacity. 1-2 GB of data are accumulated every 24 hours of acquisition.

When the event rate is too high, an ADC buffer is overwritten and some samples are lost, resulting in dead time. The time captured for each trigger can also be counted as dead time, as we assume each capture includes only one event and would therefore miss a second event within the captured time. Together these amount to less than one percent of the running time.

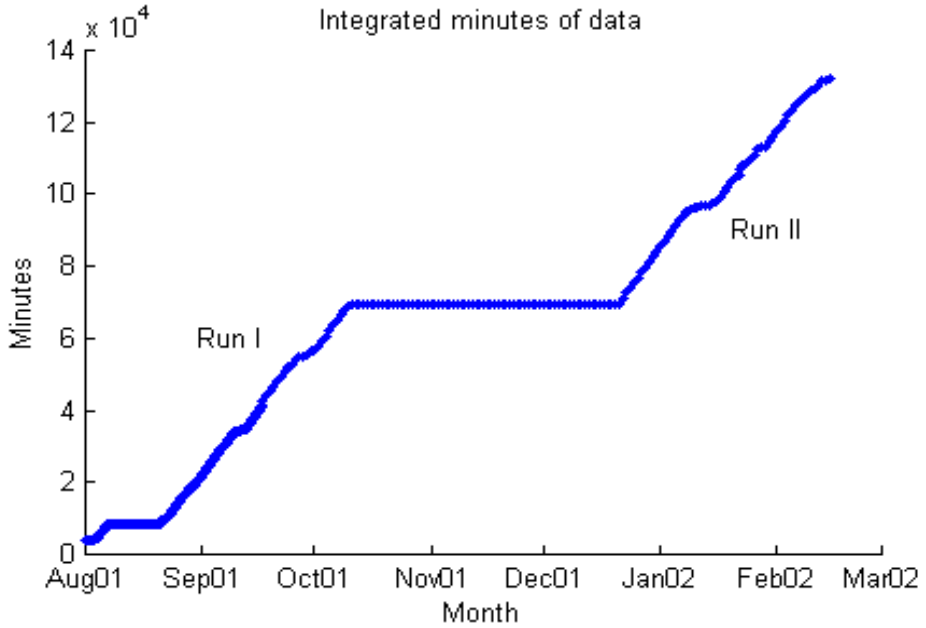

Figure 7. Integrated minutes of data (our version of integrated luminosity).

DATA OVERVIEW

Two runs have been made, one following installation of the DAQ system in August 2001 and one following the upgrade in December 2001 (Figure 7). Each run consists of roughly 70,000 minutes of data (equivalent to 1.5 months of continuous running) containing 6 million events occupying 70 GB of disk space.

In analyzing the data, two goals have been pursued: first, to achieve a low energy threshold with high efficiency and low background rate for single-phone detection of neutrino signals, and second, to detect single acoustic events with multiple channels (coincidence).

The first goal has been achieved. The distribution of trigger thresholds as determined by enforcing a 1 Hz event rate (Figure 6) reflects the empirical background rate at the experimental site. The noise consists of two types: a Gaussian background determined by weather conditions (wind produces waves at the surface that together act as a plane source, producing noise at the sea floor); and non-Gaussian acoustic events such as clicks and squeaks produced by marine animals. The Gaussian noise is fairly easily predicted a priori[11], but the non-Gaussian background event rate was previously unknown.

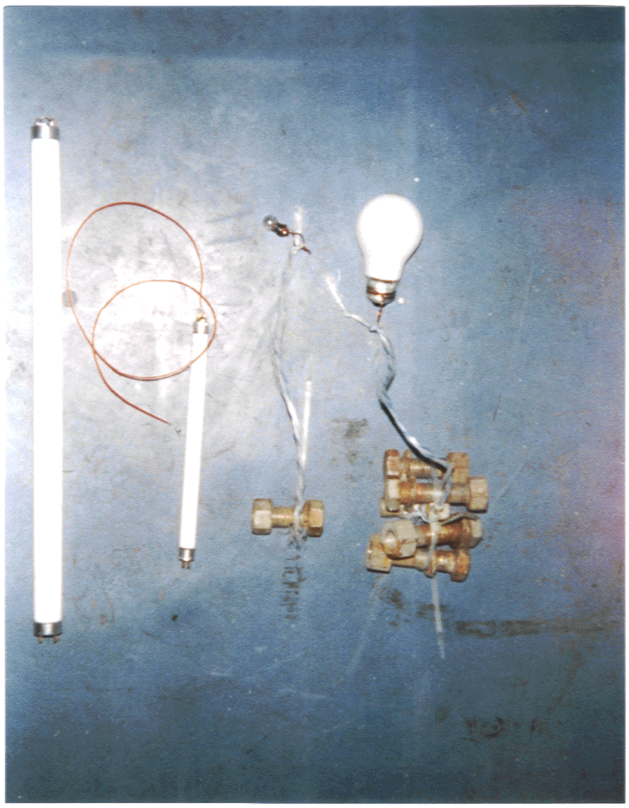

Figure 8. Calibration light bulbs.

CALIBRATION

Light bulbs are known to be a useful test source for underwater acoustics[12]. They can be weighted and sunk to implode automatically when they reach sufficient ambient pressure. Several varieties of bulbs, including 10 standard 100W bulbs (Figure 8), were weighted and dropped from a small boat over the central hydrophone. The motor of the boat was cut to reduce noise during the drops (the adaptive threshold was later seen to decrease in response). The boat was allowed to drift while the 10 bulbs were dropped, roughly once per minute. Three GPS determinations of the boat's position were made during this time.

The system captured large signals from each of the 10 bulbs (Figures 9 and 10). Each was loud enough to be detected in all seven channels. Moreover, in each channel three parts of the signal were distinguishable: a primary signal, a bottom reflection delayed ~6 ms, and a surface reflection delayed ~200 ms. These delay times are consistent with the hydrophone boom height of ~5 m and the implosion depth of ~100 m predicted from the typical failure pressure of bulbs of this type[12].

The reflection delays and the relative timing between phones were used to reconstruct each implosion event. At each phone there are three signals (a primary, a bottom reflection, and a top reflection), so we have 21 detections. At each phone, the delay between primary signal and each reflection (both top and bottom) constrains the source to a cone. The source lies at the intersection of all 14 cones, determined by

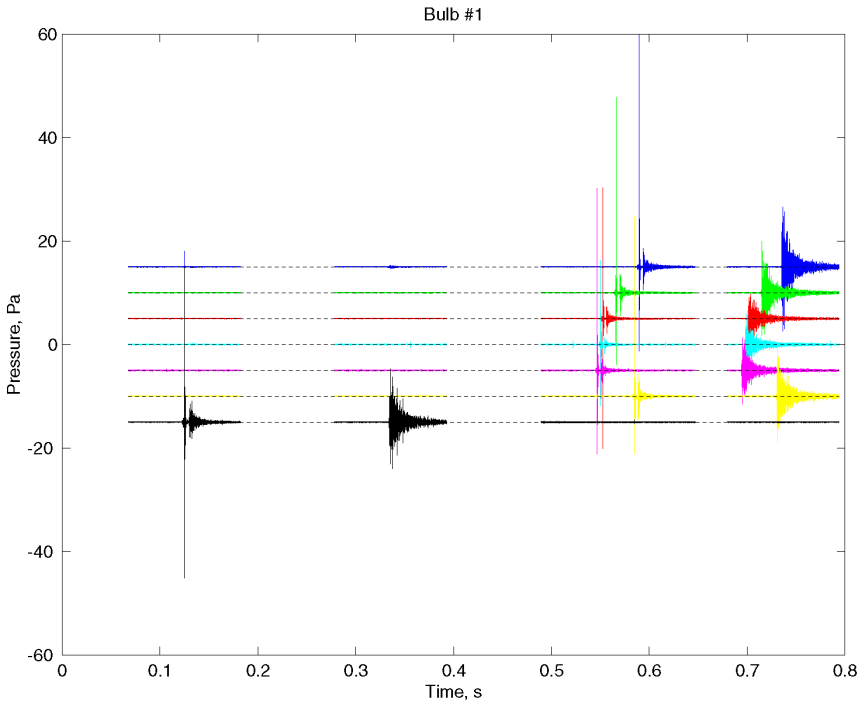

Figure 9. Acoustic signals in all channels from one bulb implosion. Each color represents a different channel. Because the bulbs were dropped above the central phone, the signal first arrives at the central phone and then at the peripheral phones after a delay. Within each channel, there are three signals: primary (vertical lines in this plot), bottom reflection (small damped signal a few ms later), and top reflection (larger damped signal 0.3 s later). The top reflection is larger than the bottom one presumably because there is less signal transmitted through the water-air interface than the water-silt interface.

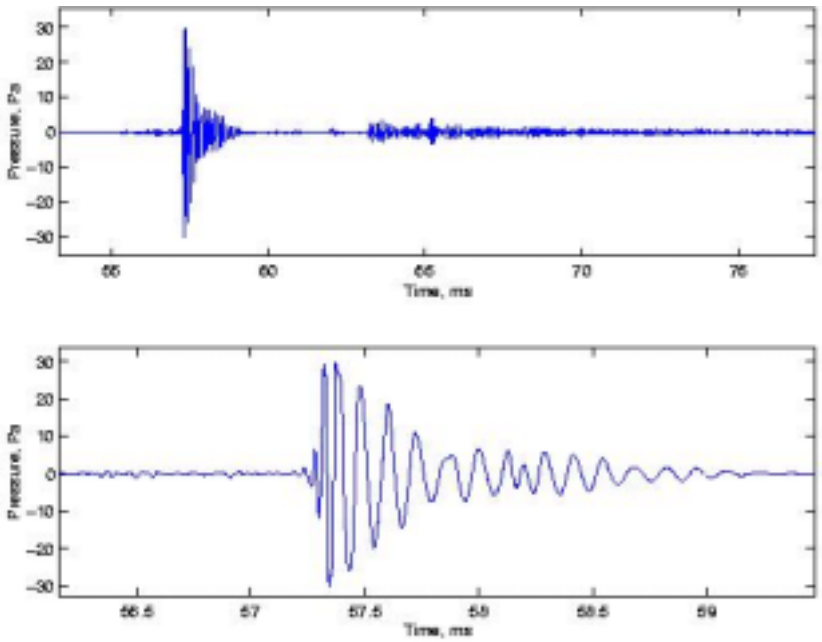

Figure 10. Close-up of central-phone signal for bulb number one. The upper plot includes the primary signal and the bottom reflection. The lower plot is a close-up of the primary signal. It is roughly a damped sinusoid.

minimizing the sum of distances squared between a test point and each cone. Using this method, the position of each bulb implosion was determined (Figure11).

The implosion pressure, P, is determined by the implosion depth, h. The pressure is that due to the weight of the water column over the bulb distributed over the area of the bulb, so $P = F/A = mg/A = \rho Vg/A = \rho gh$, where the density of water $\rho = 1000$ kg/m^3 (the density of seawater is slightly higher, but this is accurate at the part per hundred level). We can estimate the implosion energy to be PV, where the volume of the bulb $V = 0.15\times10^{-3}$ m^3. The reconstructed quantities for each bulb are given in Table 1.

The reconstructed energy is that determined from implosion depth. The energy was also determined by calculating the acoustic pulse energy (integrating the square of the pressure) and propagating it backwards to the source, accounting for divergence and absorption. This is the method with which energy would be reconstructed for a neutrino event. The energy reconstruction from this method was an order of magnitude less than that determined from implosion depth. The discrepancy is explained by the reasonable assumption that only one-tenth of the bulb's PV is converted to acoustic energy.

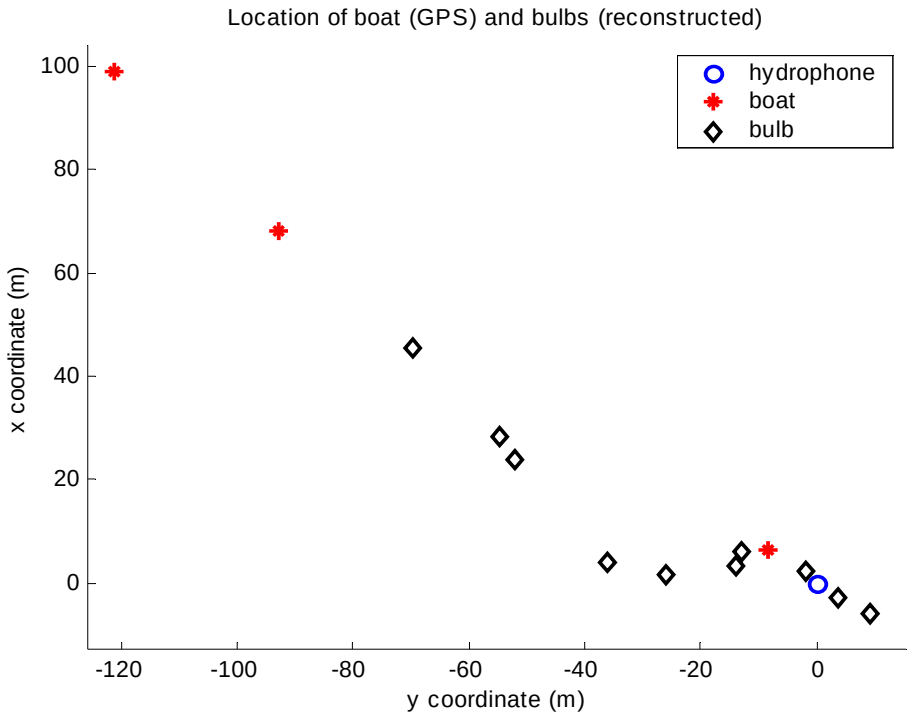

Figure 11. Light bulb position reconstructions. Coordinates are in m from central hydrophone. Stars are successive GPS measurements of the location of the boat from which bulbs were dropped. Diamonds are bulb locations as reconstructed from primary and reflection arrival times. The bulbs generally follow the path of the boat with a small lag. This is consistent with the bulbs being carried by currents as they fall. There is also a small dip in the curve of successive bulbs. The smoothness of the dip seems to indicate continuous variation in currents and position reconstruction accuracy of 10 m or less.

bulb	depth (m)	P (kPa)	E0 (J)
1	160	1563	234
2	107	1047	157
3	139	1360	204
4	166	1626	244
5	126	1237	186
6	101	990	148
7	86	838	126
8	135	1324	199
9	188	1842	276
10	290	2846	427

Table 1. Reconstructed bulb implosion depths, pressures, and energies.

COINCIDENCE DETECTION

Coincidence detection (detection of the same acoustic event with multiple hydrophones) is necessary to verify that events are acoustic as opposed to electronic noise as well as to reconstruct event position, time, and energy. Four to five phones are necessary to reconstruct time and position. If surface and/or bottom reflections are detected, fewer phones are necessary. However the calibration data indicate a reflection attenuation of an order of magnitude in amplitude, placing event reflection amplitudes well below noise. No reflections have been identified in non-calibration data.

Coincidence detection is significantly more difficult with acoustic signals than with optical signals. The speed of sound in water (1500 m/s) is one 200-thousandth the speed of light. Hence optical events are instantaneous relative to acoustic events. With an array spacing L and signal propagation speed c, the window of coincidence in time is L/c. Hence for an array of given spacing the window necessary to determine acoustic coincidence is 200,000 times larger than for optical coincidence. If an acoustic array has greater spacing than an optical array, this factor is further increased by the spacing ratio. Therefore for acoustic signals simple windowing includes many more single-phone events than could have occurred from a single acoustic event.

An algorithm has nevertheless been designed for finding valid acoustic events captured from four independent triggers. Let p_i be the phone triggered by single-channel event e_i and t_i be the time of the signal's arrival at that phone. Let d_{ij} be the distance between phones p_i and p_j. For each e_i, a "candidate list" is built. The candidate list consists of e_i along with all subsequent events e_j for which $c(t_j - t_i) < d_{ij}$, where c is the speed of sound in water. A candidate list typically includes two dozen events. At this point we face a problem of combinatorics: there may be several events in the candidate list at a single phone, but only one event from each phone can be combined to form a single multiple-channel acoustic event.

The problem of determining the position of a signal source from arrival times at multiple receivers is a common one. It arises in radar, global positioning, bioacoustics, and enhanced 911 (a technology that allows 911 operators to determine the position of a cellular phone being used for an emergency call). The common method of solution is known as time-difference-of-arrival (TDOA).

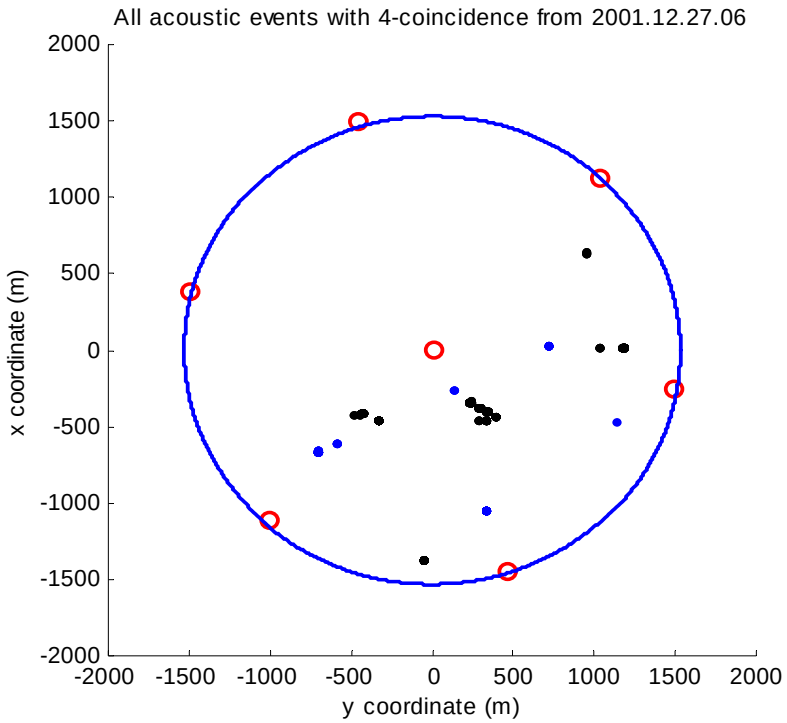

Figure 12. Acoustic events detected by four or more hydrophones from 6-7am on December 27, 2001. Blue and black color represent which of the two possible intersection points was chosen. Events are concentrated in half of the detector. It is unclear whether this is due to genuine clustering of acoustic sources or to variation among hydrophone gains.

Given n receivers, there are $n-1$ independent differences in arrival time. If receiver i is at $\mathbf{r}_i$, the signal source is at $\mathbf{s}$, the signal arrives at receiver i at time t_i, and $t_{ij} \equiv t_i - t_j$, then[13] enforcing propagation at the signal speed gives $\|\mathbf{r}_i - \mathbf{s}\|^2 = c^2 t_i^2 = c^2(t_{i1}+t_1)^2$. Each difference of arrival time determines one hyperboloid. Using four receivers gives three hyperboloid equations, which, if consistent, intersect in two points. A fifth receiver is generally necessary to distinguish between the two solutions. An exact solution of the three hyperboloid equations from four receivers exists[13].

In searching for coincidence, we restrict ourselves to triggers occurring at four nearest-neighbor phones. Four nearest neighbors in our detector form a diamond. Six such diamonds are possible, all including the central phone. If a signal is loud enough to trigger four phones that are not nearest neighbors, it should also trigger a nearest-neighbors diamond. Therefore the combinations of events from each candidate list can be restricted to those consisting of four events at four phones forming a diamond. If an acoustic source triggers more than four phones, multiple overlapping diamonds will be considered.

Each diamond determines zero (if the combination of events are not from a single acoustic source) or two intersection points. If zero, the combination is rejected. If two intersections are found, they are typically mirror sources relative to the flat array on the sea floor, one intersection lying in the sea and one below the sea floor. Intersections lying outside the cylinder determined by dragging the circle circumscribing the array (see Figure 4) from sea floor to sea surface are rejected. At this point events triggering more

than four phones result in multiple position reconstructions. These are combined for a single reconstruction.

Coincidence events are rare, not occurring in most hours of data. An hour with many acoustic coincidence events is shown in Figure 11. Rejecting events not detected by four detectors as well as those that do not match the predicted neutrino pulse shape appears to eliminate all background events.

ENERGY THRESHOLD AND EFFECTIVE AREA

A program was written by Nikolai Lehtinen to simulate the acoustic pulse produced by a hadronic shower. It uses a Monte Carlo showering package to determine the energy deposition by the shower. It then treats the energy deposition as a set of point sources and determines the signal produced at a given detection point, including the effects of divergence and absorption during propagation. The program was used to simulate the acoustic pulse resulting from a 5×10^{20} eV neutrino at an array of points representing possible hydrophone locations relative to the shower. At each point the signal was then filtered with the digital matched filter from our DAQ system.

If the filtered signal at a given point surpasses the detection threshold, the simulated event would be detected by a hydrophone at that point. An array of such points determines a contour separating the hypothetical hydrophones that detect the shower from those that do not. Equivalently, the shower can be simulated to occur at an array of points relative to a fixed hydrophone. From this point of view the contour determines a volume within which showers will be detected by a single hydrophone.

The contour depends on the value of the adaptive threshold. The effective detection volume increases with decreasing threshold. A set of contours can be drawn for various threshold values. Alternatively, we can consider the threshold to be fixed and draw a detection contour for various neutrino energies. The two are equivalent because the filtered signal (the trigger parameter) depends linearly on the acoustic pressure amplitude, which depends linearly on the neutrino energy.

For a given threshold, a detection volume can be determined for each neutrino energy. Because the threshold varies, the detection volumes vary. Figure 13 shows the detection contours for the mean threshold, 0.049. The detection volume for a neutrino of energy E can be approximated by a very flat disk of radius R, height H, area A, and volume V. The dimensions of these disks are given in Table 2.

Currently our detection threshold is limited by data rate, not noise level. More data handling capability and/or a more sophisticated DAQ algorithm may allow a lower threshold.

E (10^{19} eV)	R (m)	H (m)	A (km^2)	V (km^3)
5	200	10	0.1	0.001
10	500	10	0.8	0.008
15	800	10	2	0.02
20	1100	10	4	0.04
25	1400	10	6	0.06

Table 2. Approximate detection dimensions for a single hydrophone.

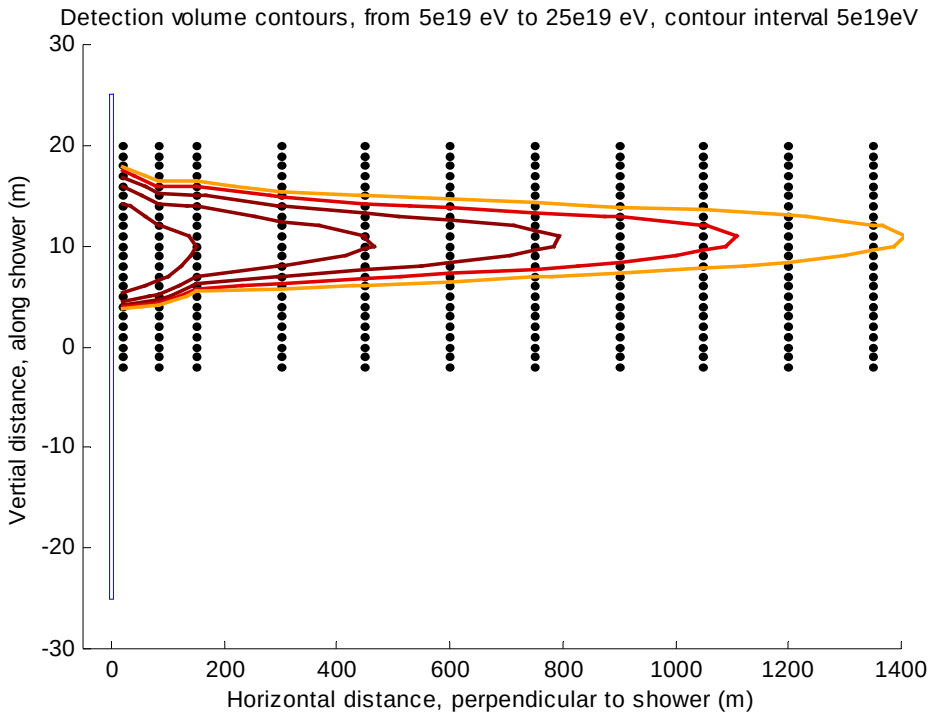

Figure 13. Detection contours for five neutrino energies, (5-25)×10^{19} eV, running with mean filter detection threshold. The blue rectangle represents the 5 m by 50 m cylinder in which the hadronic shower deposits energy. This deposition is seen to peak at 10 m. Black dots indicate hypothetical detector locations used to determine the contours. Only half of the symmetric cross section of the contours is shown (the radiation is azimuthally symmetric about the shower axis).

IDEAL ACOUSTIC ARRAY

The dimensions of the detection volume per hydrophone can be used to configure an ideal acoustic array. We require detection of a single shower by four hydrophones for position reconstruction. Consider a detector consisting of an array of strings separated by a distance *r*, each containing *p* hydrophones. For neutrinos incident from zenith, the pancake radiation is horizontal and we can have large string spacing. Detection of neutrinos with a greater zenith angle, however, requires smaller string spacing.

With an anisotropic detector, detection volume is a function of zenith angle. An ideal detector maximizes detection volume over a large solid angle. This is measured by the acceptance, defined to be the integral of detection volume over solid angle. Because the flux below 60° is less than half that at zenith (Figure 14), we configure a detector such that a 10^{20} eV neutrino will trigger four hydrophones if incident at $\theta_0 = 60°$ and more if at a smaller zenith angle, θ. A detection area *A* projected onto the horizontal plane (perpendicular to the strings) has area $a = A\cos(\theta)$. Therefore we want a detector with four strings per $A\cos(\theta_0) = A/2$, or one string per $A/8$. We assume the hydrophone spacing within strings is small enough that a detection volume with $\theta < \theta_0$ intersecting a string will intersect a hydrophone on that string. In an equilateral array with spacing r, the area per string is $r^2\sqrt{3}/2$. So we want $r^2 = A/4\sqrt{3}$. Using *A* of order 1 km^2 for

10^{20}eV, this gives $r \approx 400$ m, an order of magnitude greater than that used in optical arrays. To determine the hydrophone spacing on each string, the worst case is a horizontal detection volume from a neutrino at zenith. To detect this case we need spacing of 10 m.

A detector with 500 strings could achieve 100 km^2-scale area. It is difficult, however, to achieve a sufficient length of strings with 10 m hydrophone spacing. The interaction length of neutrinos in water at this energy is 100 km[14]. Presently conceivable detectors are 1-2 km or less in depth, much less than the interaction length. In this thin-detector regime, the detection rate is proportional to the height of the detector. An ideal detector element would be a very long, continuous string that could detect acoustic signals arriving anywhere along its length.

An undersea optical-acoustic hybrid array is conceivable. A purely optical trigger could initiate passive acoustic capture. Capturing events with both methods would allow for calibration of the acoustic method with the well-known optical method. Unfortunately, a hybrid array would be constrained to areas typical of the optical method. The energy threshold for acoustic detection is likely too high to yield a practical event rate with this area.

Perhaps more promising is the possibility of a hybrid array in ice. Acoustic signals are believed to propagate with low attenuation in Antarctic ice[15]. Logistics are challenging, but a large under-ice neutrino detector is already established (AMANDA), with a next-generation detector funded (IceCube). Members of the AMANDA/IceCube collaboration are interested in installing a small acoustic array.

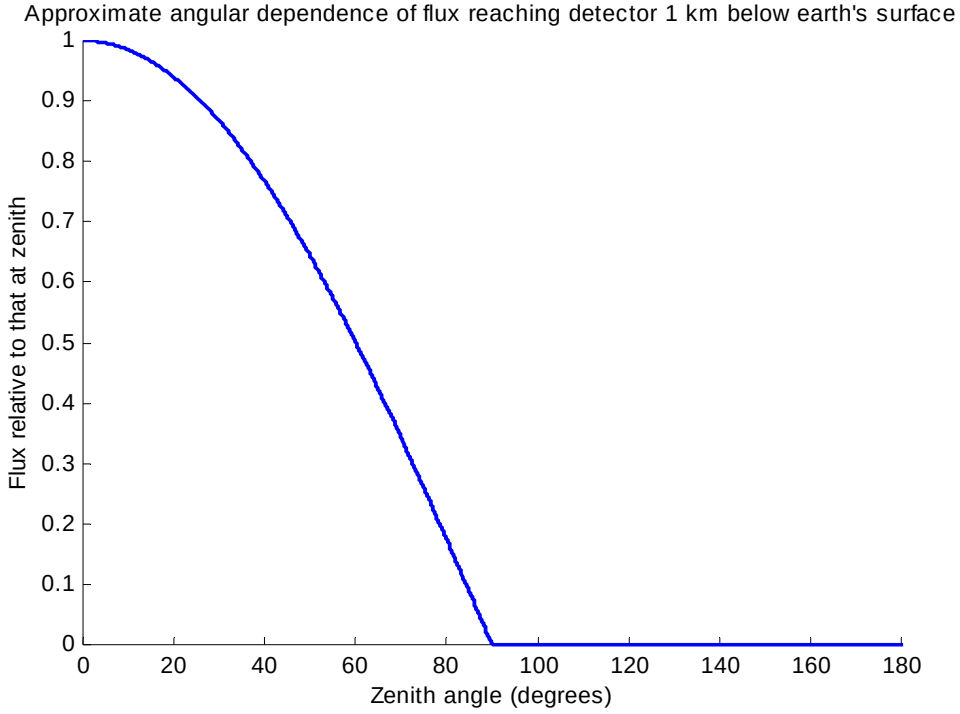

Figure 14. Angular dependence of flux arriving at an underground detector due to interaction in the Earth.

CONCLUSION

Relative to other methods, undersea acoustic detection of EHECR neutrinos benefits from a high duty cycle with low dead time and a large effective area. It suffers from the flatness of the radiation pattern and the difficulty of coincidence detection due to the slow speed of sound. To explore these factors in detail, an acoustic array has been equipped for EHECR neutrino detection and has accumulated data for several months. Multiple-phone coincidence detection has been achieved and used to greatly reduce the background. Coincidence detection has been used to reconstruct event position, time, and energy of test signals and background events. The effective detector volume and area using this method have been determined for relevant energies. An effective area of order 100 km^2 can be achieved with 500 detector strings. This is more strings than ideal but is favorable relative to optical arrays, which require 100 times as many strings for a similar area. As our study is data-rate limited rather than noise-limited, a larger project with greater data-rate capabilities and/or a more sophisticated DAQ algorithm could likely achieve a lower threshold, resulting in a greater detection area per string and making a larger detector more feasible. With a very large detector, the mystery of EHECR could be solved. The explanation will likely be very interesting to both astrophysicists and particle physicists. Perhaps it will usher in a new era of discoveries in particle physics, as the explanation of low-energy cosmic rays did 70 years ago.

ACKNOWLEDGEMENTS

I would like to thank Giorgio Gratta at Stanford University for encouraging me, supporting me, and challenging me to take on large responsibilities in the study as an undergraduate; Nikolai Lehtinen, now at the University of Hawaii, for explaining various theoretical issues and offering valuable feedback on my ideas; Jack Cecil at AUTEC for enthusiastically facilitating our use of the array; and Daniel Belasco at AUTEC for running the data acquisition system at Site 3.

---

[1] Much of this history is taken from M. S. Longair, *High Energy Astrophysics*. New York: Cambridge University Press, 1983.

[2] D. H. Perkins, Introduction to High Energy Physics, 4th ed. Cambridge: Cambridge University Press, 2000.

[3] http://astroparticle.uchicago.edu/cosmic_ray_spectrum_picture.htm

[4] K. Greisen, "End to the cosmic ray spectrum?" Phys. Rev. Lett. **16**, 748-750 (1966).

G. T. Zatsepin and V. A. Kuzmin, "Upper limit of the spectrum of cosmic rays," JETP Lett. **4**, 78-80 (1966).

[5] Originally published in M. Takeda *et al*, "Observation of the cosmic_ray energy spectrum beyond the predicted Greisen-Zatsepin-Kuz'min cutoff," Phys. Rev. Lett. **81,** 1163-1166 (1998); updated in Ref. 6.

[6] http://www-akeno.icrr.u-tokyo.ac.jp/AGASA/results.html

[7] G. Sigl, "Ultrahigh energy neutrinos and cosmic rays as probes of new physics." *hep-ph/0109202*.

[8] L. A. Anchordoqui, J. L. Feng, H. Goldberg, and A. D. Shapere, "Black holes from cosmic rays: probes of extra dimensions and new limits on TeV-scale gravity." hep-ph/0112247.

[9] J. G. Learned, "Acoustic radiation by charged atomic particles in liquids: an analysis," Phys. Rev. D. **19**, 3293-3296 (1979).

[10] L. Sulak *et al*, "Experimental studies of the acoustic signature of proton beams traversing fluid media," Nucl. Instr. Meth. **161**, 203-217 (1979).

[11] N. G. Lehtinen *et al*., "Sensitivity of an underwater acoustic array to ultra-high energy neutrinos." *astro-ph/0104033*.

[12] G. J. Heard GJ, M. McDonald, N. R. Chapman et al, "Underwater light bulb implosions: a useful acoustic source," Proc. IEEE Oceans 1997, 755-762 (1997).

[13] J. Spiesberger, "Hyperbolic location errors due to insufficient numbers of receivers," J. Acoust. Soc. Am. **90**, 3076-3079 (2001).

[14] R. Gandhi, C. Quigg, M. H. Reno, and I. Sarcevic, "Neutrino interactions at ultrahigh energies," Phys. Rev. D. **58**, 093009 (1998).

[15] P. B. Price, "Mechanisms of attenuation of acoustic waves in Antarctic ice," Nucl. Instrum. Meth. A. **325**, 346-356 (1993).